



Positron annihilation study on CuInSe₂ solar cell thin films

Lijuan Zhang^a, Tao Wang^b, Ji Li^c, Yingping Hao^a, Jiandang Liu^a, Peng Zhang^d, Bin Cheng^a, Zhongwei Zhang^c, Baoyi Wang^d, Bangjiao Ye^{a,*}

^a Department of Modern Physics, University of Science and Technology of China, Hefei 230026, China

^b Institute of Fluid Physics, CAEP, P.O. Box 919-106, Mianyang 621900, China

^c Department of Materials Science and Engineering, University of Science and Technology of China, Hefei 230026, China

^d Key Laboratory of Nuclear Analysis Techniques, Institute of High Energy Physics, Chinese Academy of Sciences, No. 19 Yuquan Lu, Beijing 100049, China

ARTICLE INFO

Article history:

Received 12 February 2012

Received in revised form 12 October 2012

Accepted 12 October 2012

Available online 29 October 2012

Keywords:

Copper indium selenide

Annealing

Positron annihilation

Defect layer

ABSTRACT

Positron annihilation spectroscopy has been used to investigate CuInSe₂ solar cell thin films. The films were grown on Mo-coated soda lime glass substrates by the electrochemical deposition processing technique. As-grown samples are found to contain large concentration of vacancy defects. The selenium (Se) atmosphere and sulfur (S) atmosphere annealing of as-grown samples at 800 K can dramatically reduce the number of vacancy defects and the film becomes crystalline. In addition, a defect layer of about 50 nm thickness was observed at the surface of the CuInSe₂ thin film. This layer results from the electrochemical deposition method, but the defect concentration in the defect layer can be greatly reduced by annealing in selenium atmosphere. The Doppler broadening line shape parameter correlation plot provided evidence that the positron trapping defect states where in three samples.

Crown Copyright © 2012 Published by Elsevier B.V. All rights reserved.

1. Introduction

Chalcopyrite semiconductors are suitable materials for optoelectronic devices due to their direct band gaps. So far, they have been mainly used as absorber materials in polycrystalline thin film solar cells. The thickness of the required layer is often below 2 μm, contributing to the potential for this technology to produce cheap photovoltaic devices. CuInSe₂ (CIS) and its derivative Cu(In,Ga)Se₂ have been used as absorber for high efficiency photovoltaic devices which result in stable device performance [1–5]. The conversion efficiency of laboratory thin film CIS-based solar cells has surpassed 20% [6,7]. CuInSe₂ has a direct band gap of about 1.05 eV that is close to the optimum band gap for solar cell of $E_{g,opt} = 1.35$ eV, as it was calculated by Henry [8] for terrestrial conditions. Compared to the other known semiconductors, CIS has the highest absorption coefficient; it exceeds 10^5 cm⁻¹ [9].

The electric properties of polycrystalline CIS thin film solar cell are strongly influenced by the presence of defects [10,11]. These defects include native point defects (vacancies, divacancies, interstitials, etc.) and extended defects (dislocations, grain boundaries, etc.) that result from deviations from the stoichiometric composition caused by the preparation process. The defect physics of CIS is known to be complicated due to the great number of native defects and complex defects [12]. However, understanding of the performance of CIS requires knowledge about defects which are expected to dominate its properties.

Positron annihilation spectroscopy (PAS) performed using a monoenergetic positron beam with variable energy, is well suited to the non-destructive study of stoichiometry defects in thin films due to its sensitivity and selectivity to vacancy defects [13–15]. In recent years, a lot of significant results have been achieved by applying positron annihilation techniques into thin film defect studies [12,16–19]. For the purposes outlined in the work, we employed two different positron annihilation spectroscopies: variable-energy positron annihilation lifetime spectroscopy and Doppler broadening spectroscopy coupled to a slow mono-energy positron beam.

2. Experimental details: sample preparation and positron annihilation spectroscopy

In this section, we present the sample preparation firstly and then, the details of PAS experiments will be given. The CuInSe₂ samples studied in this work were grown by the electrochemical deposition processing technique described in detail elsewhere [20,21]. The CIS thin films were electrodeposited on Mo coated soda-lime glass substrates. Three electrode systems with aquatic solutions containing the analytical reagents CuSO₄, In₂(SO₄)₃, H₂SeO₃, and Na₂SO₄ were used. The concentration of solution was chosen to be 3 mmol/L CuSO₄, 3 mmol/L In₂(SO₄)₃, 5 mmol/L H₂SeO₃, and 0.1 mol/L Na₂SO₄ which was chosen to be the supporting electrolyte. The solution pH value was adjusted to 2.2 by the addition of H₂SO₄. Electrodeposition was carried out in a potentiostatic mode at –0.55 V vs. saturated calomel electrode using an electrodeposition station (CHI 660C). The thickness of the films was about 1 μm (Fig. 1). The as-grown CIS thin films were

* Corresponding author. Tel.: +86 551 607422.
E-mail address: bjye@ustc.edu.cn (B.J. Ye).

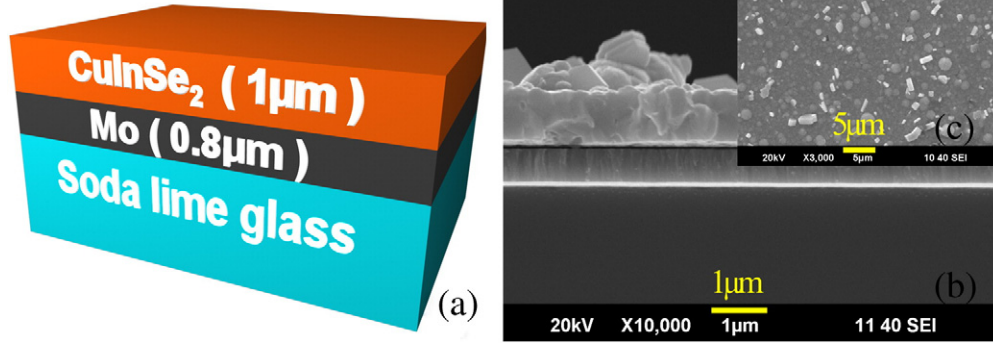


Fig. 1. Schematic drawing of the layered structure of the CuInSe₂ solar cell thin film (a), the micrograph of CuInSe₂/Mo/glass solar cell thin film cross section (b) and surface (c) was observed using scanning electron microscopy (SEM, JEOL JSM-6390LA) with an accelerating voltage of 10–15 kV.

annealed in selenium atmosphere (Se-atm) and in sulfur atmosphere (S-atm) respectively. The detailed annealing procedure was described in our previous studies [22,23]. The background pressure in the system was 10^{-1} Pa and the annealing temperature was kept at 800 K for 20 min.

PAS experiments were done at room temperature. Two PAS techniques were employed to research defects in CIS thin film, using radioactive ²²Na isotopes as a positron source. Firstly, we discuss briefly the positron lifetime experiments, which employed a pulsing positron beam system from the IHEP, China [24–26]. The positron beam based lifetime system is an improved version of one described previously by Szpala et al. [27]. The time resolution was about 0.3 ns full width at half maximum and the peak-to-background ratios ranged from 300 to 600. The time window is about 26.7 ns wide with a channel width of 25 ps. The total number of counts per spectrum ranged about two million. The measurements were performed at the positron energy of 10 keV, corresponding to a mean positron implantation depth of ~300–400 nm for the bulk lifetime. After subtracting the source and background components, the lifetime spectra were fitted to the following expression:

$$L(t) = R \otimes \sum_i I_i \exp(-t/\tau_i)$$

where τ_i is one of the lifetime components of the spectra, and I_i is the corresponding intensity. Taking into account the convolution with the instrumental resolution R , the experimental data can be fitted with several positron lifetime components by the software LIFETIME 9 (J. Kansy, Inst. of Phys. Chem. of Metals, Silesian University, LIFETIME version 9.0 (June 2002)).

As a second technique, we carried out Doppler broadening spectrometry by measuring the positron–electron momentum distribution at room temperature coupled to a slow positron beam. Doppler broadening spectra of positron annihilation radiation are characterized by S and W parameters. The S -parameter mainly reflects the change due to the annihilation of positron–electron pairs with a low-momentum distribution while the W -parameter for high-momentum distribution. The low- S and high- W momentum annihilation fractions in our experiments were measured in the momentum range $(0-2.80) \times 10^{-3} m_0c$ and $(10.5-26) \times 10^{-3} m_0c$, respectively, whatever the value of the positron energy. The S and W values were recorded as a function of the positron energy E_p between 0.07 and 20.0 keV using a slow positron beam. For the keV energy of positron, the probability of its implantation depth is given by [28,29]

$$P(z, E) = \frac{m \left[\rho \Gamma \left(1 + \frac{1}{m} \right) \right]^m z^{m-1}}{(AE^n)^m} \exp \left\{ - \frac{\left[\rho \Gamma \left(1 + \frac{1}{m} \right) \right]^m z^m}{(AE^n)^m} \right\}$$

where P is the probability of positron implantation depth, m is the shape parameter, z is the depth from the surface, E is the energy of the positron, and ρ is the material density. In addition, the empirical parameters $A \approx 400$, $m = 2$ and $n = 1.6$. The positron mean implantation depth in CIS varied from 0 to 1200 nm in this energy range. The positron implantation profiles are represented in Fig. 2 for several positron incident energies in the range $E = 1.5-20$ keV.

3. Results and discussion

Fig. 3 depicts the positron lifetime spectra of these three samples measured using the positron beam implantation energy of 10 keV. It shows a shorter positron lifetime for the annealed films, consistent with the reduction in the size and/or concentration of positron trapping defects. The analysis revealed that the spectra consist of only one lifetime component and the reduced variances of fit (χ^2) were in the range of 1.0–1.2 for the analyses. Table 1 lists the bulk lifetime of experimental measurements (as-grown, Se-atm and S-atm) and theoretical calculation [30]. Obviously, the bulk lifetime is lessened by the selenium atmosphere and sulfur atmosphere annealing. The observed lifetime of Se-atm is close to the value that has been obtained for the divacancies in CuInSe₂, from the theoretical calculation of the positron lifetimes in Ref. [30] and Ref. [31] (see Table 2). The

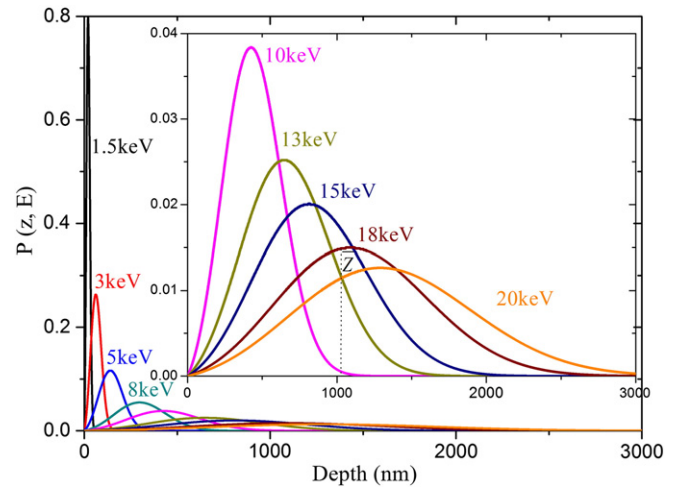


Fig. 2. Positron depth profile in CuInSe₂ calculated for indicated positron incident energies according to Ref. [29] and Ref. [30] with the parameters $\rho = 5.77$ g/cm³, $m = 2$, $n = 1.6$ and $A = 400$. The inset shows a zoom of the data in the main panel, for positron incident energies between 10 and 20 keV. The dashed line in the inset indicates the mean penetration depth z for 18 keV.

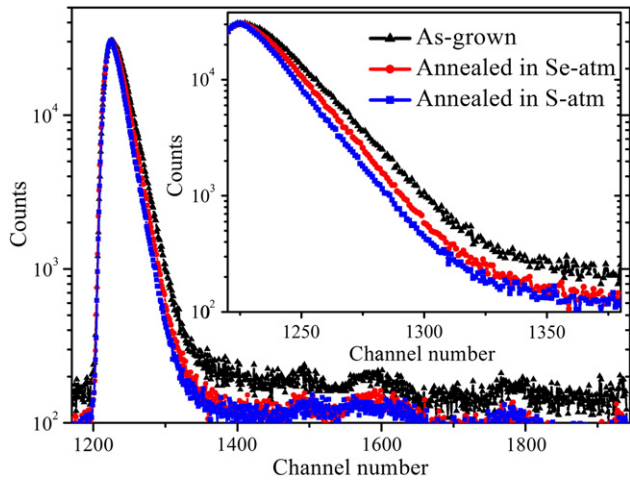


Fig. 3. Positron lifetime spectra of these samples (as-grown, Se-atm and S-atm) at $E = 10$ keV. The inset shows a zoom of the data in the main panel, for channel number between 1200 and 1280.

lifetime of S-atm (276 ps) suggests the presence of smaller vacancy defects in the sample.

Fig. 4 shows the variation of the positron annihilation Doppler broadening S -parameter as a function of incident positron beam energy E_p for the three samples (the W - E curves mirror the S - E data and are not shown here). The S -parameter profile reflects the structure of the layered CIS/Mo/glass solar cell system. Up to positron energies of 18 keV (corresponding to about $1 \mu\text{m}$ mean implantation depth in Fig. 2), the S -parameter can be assigned to the CIS layer. The variation of S at low energies ($E < 4$ keV) is due to positron trapping at the surface. For higher incident energies ($E > 18$ keV), S -parameter is due to annihilation in the Mo/glass substrate and is therefore not relevant for this study.

The starting value of the S -parameter corresponding to $E_p = 0.07$ keV, is characteristic of the surface and this value is initially higher for Se-atm and S-atm as compared to the as-grown sample. As the beam energy increases, positrons probe the CIS region. For the as-grown sample, the S -parameter initially increases steeply and it exhibits a broad maximum between 1 and 3 keV, beyond which it starts decreasing sharply. Then, it gradually remains steady with the $E_p > 4$ keV. In the case of Se-atm, an initial sharp reduction in S -parameter is observed and further, it holds a slow decrease between 3 and 10 keV, and gradually attains steady value beyond 12 keV. S-atm shows a similar behavior and the observed S -parameter value is lower than that of Se-atm. At higher incident beam energies (beyond 18 keV), the positrons probe deeper depths corresponding to the Mo substrate. At these sample depths, the S versus E_p curves for the all the samples tend towards the Mo substrate value.

Compared to the other two samples, the higher S -parameter observed for the as-grown sample indicates that it contains a large concentration of open volume defects. In the case of S-atm, which is annealed in sulfur atmosphere, the stoichiometric defects are further reduced, which is brought out clearly with the lowest observed S -parameter. The decrease in S -parameter observed by the positron beam with energy between 3 and 18 keV (Se-atm, S-atm) indicates that the number of these vacancy defects was reduced by the annealing

Table 1
Calculated and experimental positron lifetimes in ps.

	Theoretical calculation [28]		Experimental measurement		
	Perfect lattice		As-grown	Se-atm	S-atm
Bulk lifetime (τ)	235		459 ± 2.7	355 ± 2.6	276 ± 6.1

Table 2
Calculated positron lifetimes of different vacancies in ps.

	Lifetime [31]	Lifetime [32]
Bulk	235	240
V_{Cu}	250	262
V_{In}	257	284
V_{Se}	253	257
$V_{\text{Cu}}-V_{\text{In}}$	272	291
$V_{\text{Cu}}-V_{\text{In}}$	301	361
$V_{\text{In}}-V_{\text{Se}}$	307	328
$V_{\text{Cu}}-V_{\text{Cu}}$	–	277
$V_{\text{In}}-V_{\text{In}}$	–	298
$V_{\text{Se}}-V_{\text{Se}}$	–	278

in selenium and sulfur atmosphere. These results are consistent with the positron lifetime spectra measurements described above.

In the CIS surface region, the S -parameter decreases with the energy of the positron increasing (Se-atm, S-atm). The decrease has a strong contribution from surface effects [14,15] (i.e., annihilation of positron or positronium atoms on the sample surface). That is because the low injection energy makes most of the positrons remain in the CIS surface region, and part of the positrons diffuse back to the surface to annihilate in surface states. For this reason, with increasing of the positron energy, the decreased number of the positrons that diffuse back to the surface causes the S -parameter to gradually decrease. However, the S -parameter of the as-grown sample has an unusual variation in that it increases with the positron energy. And the S -parameters of as-grown and S-atm samples have sharply decreased when the positron energy is near 4 keV. These significant phenomena indicate that a defect layer exists in the CuInSe_2 solar cell thin film surface. The defect layer results from the electrochemical deposition. In comparison with the S-atm, annealing in selenium atmosphere can reduce a large number of defects in the defect layer.

Take into account the diffusion of the positrons in each layer, the experimental S -parameter versus E_p curves were analyzed using the code VEPFIT [32,33], by assuming a three-layer model comprising of the defects layer, bulk layer and Mo layer for each sample. The positron diffusion equation is solved to fit the experimental data, so as to deduce the S -parameter, positron diffusion lengths and boundary layer thickness corresponding to various assumed layers. The VEPFIT fitting results are plotted in Fig. 5 for a better visualization. From

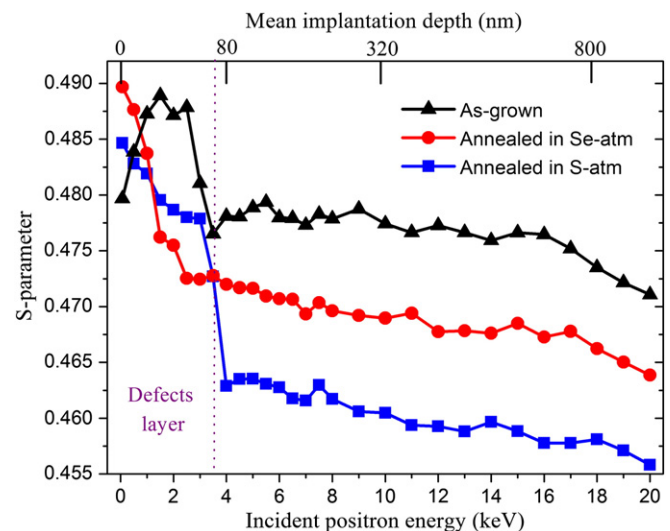


Fig. 4. Low-momentum annihilation fraction S -parameter versus incident positron energy E_p for samples of as-grown, Se-atm and S-atm. The mean positron implantation depth is shown on the top axis.

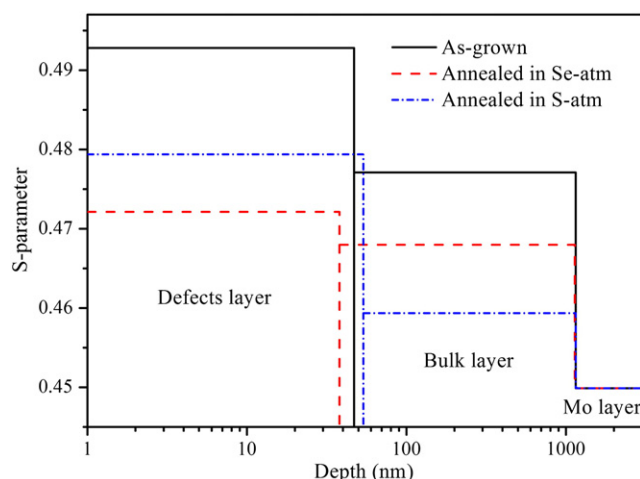


Fig. 5. Resolved S -parameter of CIS versus sample depth, extracted from VEPFIT spectra simulation. The variances of fit (χ^2) are in the range of 1.2–1.8. Samples of as-grown (solid line), Se-atm (dashed line) and S-atm (dash dotted line).

this analysis, the thickness of the defect layer in as-grown, Se-atm and S-atm samples was deduced as 47.2 ± 7 , 53.6 ± 2 and 38.0 ± 2 nm, respectively. The deduced positron diffusion lengths in the defects layer for as-grown, Se-atm and S-atm samples are found to be 2.85 ± 0.3 , 5.24 ± 0.4 and 4.36 ± 0.7 nm respectively. The shorter diffusion length in the as-grown sample signifies a larger concentration of positron trapping vacancy defects. For the other two samples, the diffusion lengths are larger but are not comparable with the bulk diffusion length (20–50 nm) observed in bulk layer. As seen in Fig. 5, the difference of S -parameter between defects layer and bulk layer is very small in the sample of Se-atm. And the sample of S-atm appears to have repaired a large fraction of the defects in the bulk layer of CIS film. This indicates that when annealing in the S-atm, the S ion is able to replace the Se ion and even occupy the Se vacancy in the CIS surface. In addition, the ionic migration activation energy of the S ion is far less than the Se ion. Thus, the S ions in the CIS surface diffuse into the bulk layer of the CIS film. The result is that (See Fig. 5), in the defect layer, the number of defects in S-atm annealing is lower than that in the as-grown sample while it is higher than that in the Se-atm annealing sample; in bulk layer, the defects of S-atm annealed sample decrease dramatically.

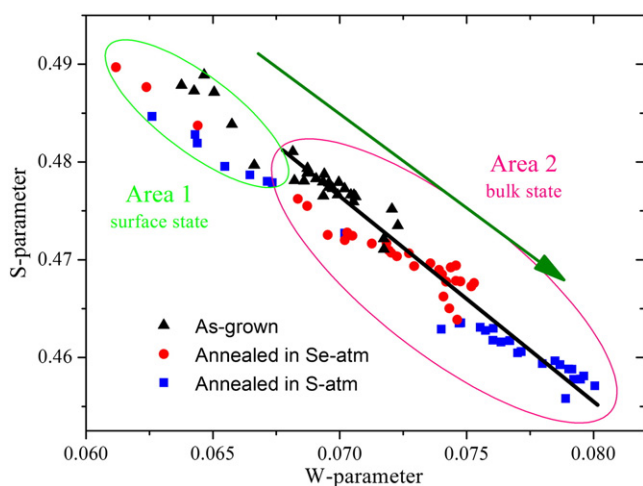


Fig. 6. Positron annihilation characteristic maps, using the low electron momentum fraction S and the high electron momentum fraction W , with the incident positron energy as a running variable for these three samples.

Positron annihilation correlation plots of the S -parameter and its complementary W -parameter are found to be useful in distinguishing various positron trapping defects [14]. As seen in Fig. 4, the CIS bulk layer is observed over positron beam energies of 4–18 keV and hence, S and W parameters over this energy range have been averaged to obtain the respective S – W values for these samples. Fig. 6 shows the S – W correlation plot for each sample. The area 1 reflects the surface state (incident positron energy below 4 keV) while the area 2 indicates the bulk state (incident positron energy between 4 and 18 keV). The S – W coordinate of the as-grown sample signifies a larger S -parameter with a lower W -parameter compared with the Se-atm and S-atm samples. It moves towards a lower S -parameter and a larger W -parameter, indicating that the positron trapping vacancy defects are reduced. The S versus W plot shows that the vacancy type is similar to that of the as-grown, Se-atm and S-atm samples since the data fall on a similar linear variation.

4. Conclusions

We have carried out positron annihilation spectroscopy study on the defects in CuInSe_2 solar cell thin films that were grown by the electrochemical deposition processing technique under different conditions: as-grown, selenium atmosphere annealed and sulfur atmosphere annealed. The defect sensitive S -parameter indicates a large concentration of defects in as-grown CIS film. The large number of open volume sites can be reduced in selenium atmosphere and sulfur atmosphere annealing of as-grown samples at 800 K. From our analysis, we have demonstrated that a highly defective surface layer of thickness approximately 50 nm exists in the CuInSe_2 solar cell thin films studied. The defect layer formation is related to the material fabrication by electrochemical deposition and the defect concentration in the defect layer can be reduced by annealing in selenium atmosphere. The linear behavior of the Doppler broadening spectroscopy line shape parameter, S – W , correlation plot provides evidence that similar positron trapping defect states are present in the three samples.

Acknowledgments

This work is supported by the State Key Program of National Science Foundation of China (grant no. 10835006) and the National Natural Science Foundation of China (grant no. 11175171).

References

- [1] B.J. Stanbery, Crit. Rev. Solid State Mater. Sci. 27 (2002) 73.
- [2] M. Kemell, M. Ritala, M. Leskelä, Crit. Rev. Solid State Mater. Sci. 30 (2005) 1.
- [3] L.L. Kazmerski, J. Electron. Spectrosc. 150 (2006) 105.
- [4] I. Repins, M.A. Contreras, B. Egaas, C. DeHart, J. Scharf, C.L. Perkins, B. To, R. Noufi, Prog. Photovolt. 16 (2008) 235.
- [5] O.C. Miredin, P. Choi, R. Wuerz, D. Raabe, Appl. Phys. Lett. 98 (2011) 103504.
- [6] M.A. Contreras, K. Ramanathan, J. AbuShama, F. Hasoon, D.L. Young, B. Egaas, R. Noufi, Prog. Photovolt. 13 (2005) 209.
- [7] P. Jackson, M. Powalla, E. Lotter, D. Hariskos, S. Paetel, R. Wuerz, R. Menner, W. Wischmann, Prog. Photovolt. Res. Appl. 19 (2011) 894.
- [8] C.H. Henry, J. Appl. Phys. 51 (1980) 4494.
- [9] M.V. Yakushev, F. Luckert, C. Faugeras, A.V. Karotki, A.V. Mudryi, R.W. Martin, Appl. Phys. Lett. 97 (2010) 152110.
- [10] C. Stephan, S. Schorr, M. Tovar, H.-W. Schock, Appl. Phys. Lett. 98 (2011) 091906.
- [11] S.H. Han, F.S. Hasoon, A.M. Hermann, D.H. Levi, Appl. Phys. Lett. 91 (2007) 021904.
- [12] F. Borner, J. Gebauer, S. Eichler, R. Krause-Rehberg, I. Dirnstorfer, B.K. Meyer, F. Karg, Physica B 273–274 (1999) 930.
- [13] P.J. Schultz, K.G. Lynn, Rev. Mod. Phys. 60 (1988) 701.
- [14] R.K. Rehberg, H.S. Leipner, Positron Annihilation in Semiconductors, Springer Verlag, Berlin, 1998.
- [15] P.G. Coleman, Positron Beams and Their Applications, World Scientific, Singapore, 2000.
- [16] Z.W. Ma, L.X. Liu, Y.Z. Xie, Y.R. Su, H.T. Zhao, B.Y. Wang, X.Z. Cao, X.B. Qin, J. Li, Y.H. Yang, E.Q. Xie, Thin Solid Films 519 (2011) 6349.
- [17] A. Gentils, O. Copie, G. Herranz, F. Fortuna, M. Bibes, K. Bouzehouane, É. Jacquet, C. Carrétéro, M. Basletić, E. Tadra, A. Hamzić, A. Barthélémy, Phys. Rev. B 81 (2010) 144109.
- [18] K. Prabakar, S. Abhaya, R. Krishnan, S. Kalavathi, S. Dash, J. Jayapandian, G. Amarendra, Nucl. Instrum. Methods Phys. Res. B 267 (2009) 1167.

- [19] X.J. Hu, J.S. Ye, H.J. Liu, S. Mariazzi, R.S. Brusa, *Thin Solid Films* 516 (2008) 1699.
- [20] R.N. Bhattacharya, *J. Electrochem. Soc.* 130 (1983) 2040.
- [21] C. Sene, M.E. Calixto, K.D. Dobson, R.W. Birkmire, *Thin Solid Films* 516 (2008) 2188.
- [22] Z.W. Zhang, J. Li, M. Wang, M. Wei, G.S. Jiang, C.F. Zhu, *Solid State Commun.* 150 (2010) 2346.
- [23] Z.W. Zhang, H.Y. Guo, J. Li, C.F. Zhu, *Chin. J. Chem. Phys.* 24 (2011) 225.
- [24] Y.Y. Ma, S.L. Pei, X.Z. Cao, P. Wang, C.F. Wei, C.X. Ma, Z.M. Zhang, S.H. Wang, B.Y. Wang, L. Wei, *High Energy Phys. Nucl. Phys.* 30 (2006) 166.
- [25] Y.Y. Ma, Ph. D. Thesis, Institute of High Energy Physics, Chinese Academy of Sciences, China, 2007.
- [26] B.Y. Wang, Y.Y. Ma, P. Wang, X.Z. Cao, X.B. Qin, Z. Zhang, R.S. Yu, L. Wei, *Chin. Phys. C* 32 (2008) 156.
- [27] S. Szpala, M.P. Petkov, K.G. Lynn, *Rev. Sci. Instrum.* 73 (2002) 147.
- [28] A. Vehanen, K. Saarinen, P. Hautojarvi, H. Huomo, *Phys. Rev. B* 35 (1987) 4606.
- [29] K.A. Ritley, K.G. Lynn, V.J. Ghosh, D.O. Welch, M. Mckeown, *J. Appl. Phys.* 74 (1993) 3479.
- [30] A. Polity, R.K. Rehberg, T.E.M. Staab, M.J. Puska, J. Klais, H.J. Moëller, B.K. Meyer, *J. Appl. Phys.* 83 (1998) 71.
- [31] R. Suzuki, T. Ohdaira, S. Ishibashi, in: 2nd World Conf. on PVSEC, Wien, 1998, p. 620.
- [32] A. van Veen, H. Schut, J. de Vries, R.A. Hakvoort, M.R. Ijpma, *AIP Conf. Proc.* 218 (1990) 171.
- [33] H. Schut, A. van Veen, *Appl. Surf. Sci.* 85 (1995) 225.